Journal of Advances and Scholarly Researches in Allied Education
Vol. XV, Issue No. 6, August-2018, ISSN 2230-7540

A Study of Thermofluidics in Fluid Flow and Heat Transfer

Ritika[1]*, Dr. Ashwini kumar[2]

[1] Research Scholar, Sunrise University

[2] Associate Professor, Sunrise University, Alwar Rajasthan

Abstract- Numerous mathematical problems can be easily addressed using arithmetic operations, which is why they are referred to as numerical approaches. Finite element theory and other fields have been greatly influenced by these approaches. Here, we've provided a brief overview of the numerical methods used in mechanical engineering to solve fluid flow and heat and mass transfer problems. These methods include such things as finite difference methods and finite element methods as well as those for boundary value problems (generally), Lattice Boltzmann methods, and those for Crank-Nicolsan scheme methods. Surface tension, coning, water dispersion, Stokes' law, gravity-capillary, and unstable free surface flows, whirling, and so on have all been explored. Additionally, we've researched boundary value and eigenvalue difficulties and established a numerical method for solving these problems. As we've shown, the performance of the mechanisms (modes) varies depending on which numerical methods are used, and these methods have been applied to several fundamental heat transfer modelling approaches. Engineering heat transfer problems can be solved using the approaches presented in this study. We contrasted our results with those from other methods for determining things like thermal conductivity, energy flux, entropy, and so on.

Keywords- Thermo fluidics, Fluid, Heat Transfer, Surface tension, water dispersion

----------X----------

INTRODUCTION

Geothermal and industrial operations, such as nuclear waste disposal, heat exchanger design, and thermal insulation, are all examples of flow and heat transmission in permeable bed/boundary systems. Fluid can be injected or sucked out of the system using a porous media. Boundary layer control relies heavily on suction. A porous coating/substrate can alter the skin friction and temperature gradient at the surface qualitatively and quantitatively, as demonstrated by Vafai and Kim (1990), Huang and Vafai (1994), and Fowler and Bejan (1995). In reality, the porous layer can work as both an insulator and a heat transfer enhancement device, depending on the application. An effective hearing aid augmentation tool has been discovered to be a porous implant. Natural waterways, such as rivers, feature gravel beds because flow is copious when there is a naturally permeable border. We know that Darcy's law (1856) governs slug flow in a permeable bed, but it's important to keep in mind that, in the absence of an external pressure gradient and for small permeability, the interior flow of the porous medium would not contribute much to the exterior clear fluid flow and thus zero filter velocity in the permeable bed may be assumed. The work of Chauhan and Vyas (1995) is particularly noteworthy. Porous beds can alter clear fluid flow through Saffman (1971) who found that for small permeability, the following equation is appropriate to compute outside flow correct to zero (K0)

$$u = \frac{\sqrt{K_0}}{\alpha}\left(\frac{\partial u}{\partial y}\right)_{y=0^+} + o(K_0)$$

There are three variables in this equation: u (fluid velocity), K0 (permeability), and (empirical constant). Because these idealised flow geometries appear as a single unit or in conjunction with other configurations, they serve as good infant models for larger scale similar complex real world systems. First traditional paper on laminar flow between two porous parallel plates was presented by Berman (1953). The flow of Newtonian and non-Newtonian fluids via porous channel/tubes was recently studied by Tsangaris et al. (2007). For practical reasons, studying heat transfer in non-Newtonian fluid flow inside channels is worthwhile. Because it gives first estimates for complex flow arrangements like journal bearings and the like, the flow inside parallel plate channels is frequently studied. Non-Newtonian fluids were studied by Lin (1979) for plane Couette flow and heat transfer. In a parallel plate channel, Sukhow et al. (1980) investigated heat transfer to

non-Newtonian fluid flow. For non-Newtonian fluids, Cotta and Ozisik (1986) studied laminar forced convection in ducts with prescribed heat flow. Power law fluid flow across parallel plates was explored by Etemad et al. (1994) for viscous dissipation effects in the entrance area heat transfer. Power law fluid flow inside a parallel plate channel with continuous heat flux was studied by Tso et al. (2010). Using a simplified Phan-Thien-Tanner fluid, Pinho and Oliveria (2000) conducted an investigation on the effects of forced convection on pipes and channels. Phan-Thien-Tanner fluid driven convection in ducts with constant wall temperatures was studied by Coehlo et al. (2000). Using a Couette-Poiseuille flow of non-linear viscoelastic fluid between parallel plates, Hashemabdi et al. (2005) studied the heat transfer of forced convection. The Couette-Poiseuille flow of the Gieskuis model between parallel plates was approximated by Raisi et al. (2008). Forced convection heat transfer of viscoelastic fluid in pipes and channels was described by Khatibi et al. (2010). For example, heat exchangers, chemical reactors, and geothermal mechanisms all rely on flow and thermal characteristics in porous media channels. Flow in channels with porous media has been studied extensively by a number of writers. In a composite channel, Vyas and Srivastava (2013) investigated the impact of radiation on MHD Couette flow. Radiative MHD Couette flow of compressible fluid in a channel with a permeable base was also studied by Vyas and Srivastava (2014). Non-Newtonian fluids flowing in channels have been the subject of several studies, including those detailed here and those referred to in the references. Most earlier research in these flow configurations has focused on the fundamental law of thermodynamics. As far, little is known about the second law of thermodynamics. Both Newtonian and non-Newtonian fluid flow in channels necessitate an entropy analysis. Solid matrix, heat exchanger, thermal insulation, electronic component cooling, and other flow patterns with numerous technological applications must be considered for their inherent thermodynamic irreversibility in order to design an optimal system. Optimizing entropy allows engineers to design thermal systems with fewer energy losses and thus the highest amount of accessible power. Entropy generation analysis can be used to optimise convective devices, according to Bejan (1982, 1996, 2002). For thermodynamic efficiency, entropy generation analysis (EGA) is an important tool since it serves as a foundation for entropy generation minimization (EGM). A significant increase in research on thermofluidic designs has occurred over the last two decades. In a porous channel with viscous dissipation, Mahmud and Fraser (2005) studied flow, thermal energy generation, and entropy generation. Entropy production for forced convection in a porous saturated circular tube with uniform wall temperature was studied by Hooman and Ejlali (2007). Couette-poisieille flow of bingham fluids between two porous parallel plates with slip circumstances was studied by Chen. and Zhu in 2008. In a parallel plate microchannel, Haddad et al. (2004) studied the entropy generation caused by laminar incompressible forced convection flow. Third-grade fluid flow with temperature-dependent viscosity in an annulus partially filled with porous material was studied by Chauhan and Kumar (2013). In parallel plate microchannels, Ibanez et al. (2013) found optimal slip flow by minimising entropy formation. An investigation of the effects of convective heating on entropy formation in a channel with permeable walls was conducted by Makinde and Eegunjobi (2013). Research by Yazdi et al. (2013) focused on decreasing entropy formation in MHD fluid flow over open parallel microchannels embedded in micropatterned permeable surfaces. Ibanez et al. (2014) found that entropy formation in a microchannel was influenced by the combination of uniform heat flow border conditions and hydrodynamic slip. In a parallel channel with a naturally permeable wall, Vyas and Srivastava (2014) studied radiative MHD compressible Couette flow. Power-law fluid with asymmetric convection cooling was studied by Lopez de Haro et al. (2014), who found that heat transfer and entropy creation occurred when the flow was parallel to the plates. MHD porous channels with hydrodynamic slip and convective boundary conditions were studied by Ibanez (2015). Generalized MHD Couette flow inside a composite duct with asymmetric convective cooling was studied by Vyas and Srivastava (2015). MHD fluid flow with dissipative Casson properties in a porous media was studied by Vyas and Khan (2016) using entropy analysis to determine the amount of energy dissipated. A coupled-convection flow through a vertical channel partially filled with porous medium, with injection/suction and slip boundary conditions, was studied by Chauhan and Khemchandani (2016) using entropy analysis. In the literature, many theoretical models of convective flux with uniform convection coefficient have been presented. Nonlinear heat transfer coefficients are not always possible to achieve in some situations, hence idealisation of a uniform heat transfer coefficient is not always possible. Power law type temperature dependence or weak temperature dependence can be observed in the cooling process. The heat convection mechanism is largely temperature dependent, as has been empirically discovered. The temperature-dependent convection process has been studied by a number of researchers in a variety of fields. Straight fin heat transfer was described in 1951 by Ghai. For straight fins, Ghai and Jakob (1950) investigated local coefficients of heat transmission. Different cooling fins with temperature-dependent heat transfer coefficients were studied by Laor and Kalman (1996). A thorough review of the literature found that the uniform heat transfer coefficient was taken into account in the majority of the entropy generation studies for convective flux problems. Taking into account temperature-dependent convection, we conducted an entropy analysis to create a more realistic model and fill the gap.

SUCTION EFFECTS ON HEAT TRANSFER AND ENTROPY GENERATION IN THE FLOW OVER A POROUS BED

Mathematical model

A viscous incompressible fluid flowing with free stream velocity U(t) over a naturally permeable bed with very little permeability exhibits a non-steady flow. Suction is applied to the bed in a variety of ways. It is expected that (x,y) axes are taken along the bed and normal to it, as shown in figure 1, as indicated in the picture. The free stream uniform temperature is assumed to be and the porous strata is subjected to a uniform heat flux $T_{\infty *}$.

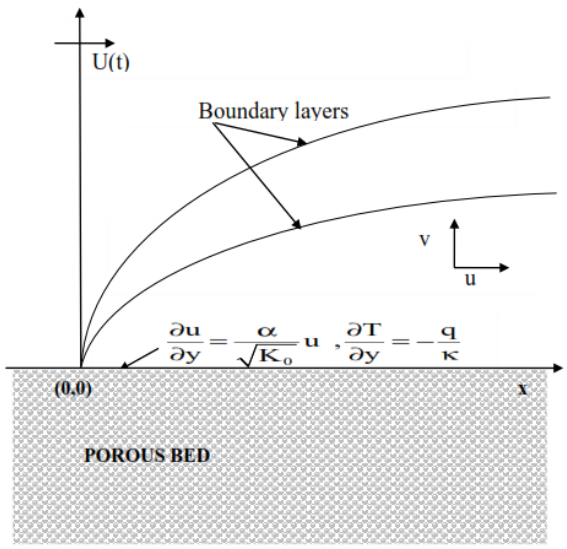

Figure 1: Schematic diagram

All other characteristics, save for pressure, are unaffected by the size of the porous strata. Setup equations are governed by these equations.

$$\frac{\partial u}{\partial t}+v\frac{\partial u}{\partial y}=-\frac{1}{\rho}\frac{\partial p}{\partial x}+\nu\frac{\partial^2 u}{\partial y^2} \quad (2.2.1)$$

$$\frac{\partial v}{\partial t}=-\frac{1}{\rho}\frac{\partial p}{\partial y} \quad (2.2.2)$$

$$\frac{\partial v}{\partial y}=0 \quad (2.2.3)$$

$$\rho C_p\left(\frac{\partial T}{\partial t}+v\frac{\partial T}{\partial y}\right)=\kappa\frac{\partial^2 T}{\partial y^2}+\mu\left(\frac{\partial u}{\partial y}\right)^2 \quad (2.2.4)$$

where (u,v) are the components of velocity in the (x,y) directions respectively, The fluid's thermal conductivity is determined by the following equations: p is pressure, is density, v is kinematic viscosity, t is time, and T is temperature. and C_p is the specific heat at constant pressure. Equation (2.2.3) suggests that v is independent of y and consequently it is a function of time only. We assume that

$$v=-V_0\left(1+\varepsilon A e^{\gamma t}\right) \quad (2.2.5)$$

where V0 is the velocity of suction at the porous bed, γ is the accelerating factor and εA is assumed to be very small quantity.

The boundary conditions are

$$\left.\begin{array}{l} y=0:\ \frac{\partial u}{\partial y}=\frac{\alpha}{\sqrt{K_0}}u\ ,\frac{\partial T}{\partial y}=-\frac{q}{\kappa} \\ y\to\infty: u\to U(t)\ ,\ T\to T_\infty \end{array}\right\} \quad (2.2.6)$$

is a dimensionless constant that depends on the structure of porous media, and K0 measures how permeable a material is. The heat flux is denoted by the symbol Q. Foam metal with average pore sizes of 0.016, 0.034, and 0.045 inches had slip coefficients of 0.78, 1.45, and 4.0, respectively, according to Beavers-Joseph (1967). It's important to remember that has nothing to do with fluid viscosity, but rather depends on the interface flow direction, Reynolds number, the volume of transparent fluid, and any known uniformities in the solid material arrangements at the permeable surface. Various values of have been empirically determined without impacting the porous medium's permeability or bulk porosity, it's worth noting. Thus, we are able to make use of as an optional parameter in porous medium-based configurations. In order to calculate the main stream's equation, we use

$$-\frac{1}{\rho}\frac{\partial p}{\partial x}=\frac{dU(t)}{dt} \quad (2.2.7)$$

Using (2.2.7) in equation (2.2.1), we have

$$\frac{\partial u}{\partial t}+v\frac{\partial u}{\partial y}=\frac{dU(t)}{dt}+\nu\frac{\partial^2 u}{\partial y^2} \quad (2.2.8)$$

we assume

$$U(t)=U_0\left(1+\varepsilon e^{\gamma t}\right) \quad (2.2.9)$$

$$u=U_0\left\{f_1(y)+\varepsilon f_2(y)e^{\gamma t}\right\} \quad (2.2.10)$$

U0 is the mean U(t) and can be taken as any positive quantity by selecting the appropriate origin.

The following non-dimensional quantities are introduced:

$$\eta=\frac{y|V_0|}{\nu}\ ,\lambda=\frac{\nu\gamma}{V_0^2},K^*=\frac{K_0}{\left(\frac{\nu}{V_0}\right)^2},t^*=\frac{tV_0^2}{\nu},$$
$$\theta=\frac{(T-T_\infty)\kappa V_0}{q\nu},ul=\frac{u}{U_0} \quad (2.2.11)$$

We also assume that non-dimensional temperature θ is as follows:

$$\theta = \theta_1(\eta) + \varepsilon e^{\lambda t^*}\theta_2(\eta) + \varepsilon^2 e^{2\lambda t^*}\theta_3(\eta)$$

using (2.2.5) and (2.2.9) to (2.2.12) in equations (2.2.4) and (2.2.8) and comparing the coefficients of various powers of te ∗ λ, we arrive at the following results:

$$\frac{d^2f_1}{d\eta^2} + \frac{df_1}{d\eta} = 0 \qquad (2.2.13)$$

$$\frac{d^2f_2}{d\eta^2} + \frac{df_2}{d\eta} - \lambda f_2 = -\lambda - A\frac{df_1}{d\eta} \qquad (2.2.14)$$

$$\frac{d^2\theta_1}{d\eta^2} + \Pr\frac{d\theta_1}{d\eta} = -\mathrm{Br}\left(\frac{df_1}{d\eta}\right)^2 \qquad (2.2.15)$$

$$\frac{d^2\theta_2}{d\eta^2} + \Pr\frac{d\theta_2}{d\eta} - \Pr\lambda\theta_2 = -A\Pr\frac{d\theta_1}{d\eta} - 2\mathrm{Br}\left(\frac{df_1}{d\eta}\right)\left(\frac{df_2}{d\eta}\right) \qquad (2.2.16)$$

$$\frac{d^2\theta_3}{d\eta^2} + \Pr\frac{d\theta_3}{d\eta} - 2\Pr\lambda\theta_3 = -A\Pr\frac{d\theta_2}{d\eta} - \mathrm{Br}\left(\frac{df_2}{d\eta}\right)^2 \qquad (2.2.17)$$

where

$$\Pr = \frac{\mu C_p}{\kappa},\ \mathrm{Br} = \frac{\mu U_0^2 V_0}{q\nu}$$

Are Prandtl number and Brinkman number.

The corresponding boundary conditions are

$$\left.\begin{aligned} &\eta = 0: \frac{df_1}{d\eta} = \frac{\alpha}{\sqrt{K^*}}f_1, \frac{df_2}{d\eta} = \frac{\alpha}{\sqrt{K^*}}f_2, \theta_1' = -1, \theta_2' = 0 = \theta_3' \\ &\eta \to \infty: f_1 = 1 = f_2, \theta_1 = \theta_2 = \theta_3 = 0 \end{aligned}\right\} \qquad (2.2.18)$$

Solution

On solving equations (2.2.13) to (2.2.17) , under the boundary conditions (2.2.18) , we obtain

$$f_1 = 1 - \left(\frac{\alpha}{\alpha + \sqrt{K^*}}\right)e^{-\eta}$$

$$f_2 = 1 + \frac{A\alpha}{\lambda\left(\alpha + \sqrt{K^*}\right)}e^{-\eta} - \frac{2\alpha(A+\lambda)}{\lambda\left\{2\alpha + \sqrt{K^*}\left(1+\sqrt{1+4\lambda}\right)\right\}}e^{-\left(\frac{1+\sqrt{1+4\lambda}}{2}\right)\eta}$$

$$\theta_1 = \frac{e^{-\Pr\eta}}{\Pr} + \frac{\mathrm{Br}\alpha^2}{\left(\alpha+\sqrt{K^*}\right)^2(4-2\Pr)}\left(\frac{2}{\Pr}e^{-\Pr\eta} - e^{-2\eta}\right)$$

$$\theta_2 = \frac{2}{\Pr + \sqrt{\Pr^2 + 4\Pr\lambda}}\left\{\frac{a'_{11}}{\lambda} - \frac{2a_{12}}{(4-2\Pr-\Pr\lambda)} - \frac{a_{13}}{a_{14}}\left(\frac{3+\sqrt{1+4\lambda}}{2}\right)\right\}\times$$
$$e^{-\left(\frac{\Pr+\sqrt{\Pr^2+4\lambda\Pr}}{2}\right)\eta} - \frac{a'_{11}}{\Pr\lambda}e^{-\Pr\eta} + \frac{a_{12}}{(4-2\Pr-\Pr\lambda)}e^{-2\eta} + \frac{a_{13}}{a_{14}}e^{-\left(\frac{3+\sqrt{1+4\lambda}}{2}\right)\eta}$$

$$\theta_3 = \frac{2}{\Pr + \sqrt{\Pr^2 + 8\Pr\lambda}}\left\{\begin{matrix}\frac{a'_{15}}{\Pr\lambda}\left(\frac{\Pr+\sqrt{\Pr^2+4\Pr\lambda}}{2}\right) - \frac{Aa'_{11}\Pr}{2\lambda^2} - \\ \frac{2a_{18}}{(4-2\Pr-2\Pr\lambda)} - \frac{a_{16}}{a_{19}}\left(1+\sqrt{1+4\lambda}\right) - \\ \frac{a_{17}}{a_{20}}\left(\frac{3+\sqrt{1+4\lambda}}{2}\right)\end{matrix}\right\}\times$$
$$e^{-\left(\frac{\Pr+\sqrt{\Pr^2+8\lambda\Pr}}{2}\right)\eta} - \frac{a'_{15}}{\Pr\lambda}e^{-\left(\frac{\Pr+\sqrt{\Pr^2+4\lambda\Pr}}{2}\right)\eta} + \frac{Aa'_{11}}{2\lambda^2}e^{-\Pr\eta} + \frac{a_{18}}{(4-2\Pr-2\Pr\lambda)}e^{-2\eta}$$
$$+\frac{a_{16}}{a_{19}}e^{-\left(1+\sqrt{1+4\lambda}\right)\eta} + \frac{a_{17}}{a_{20}}e^{-\left(\frac{3+\sqrt{1+4\lambda}}{2}\right)\eta}$$

where the constants are found to be as follows

$$a'_{11} = \Pr A\left\{1 + \frac{2\mathrm{Br}\alpha^2}{\left(\alpha+\sqrt{K^*}\right)^2(4-2\Pr)}\right\}$$

$$a_{12} = \frac{2\mathrm{Br}\alpha^2 A}{\left(\alpha+\sqrt{K^*}\right)^2}\left\{\frac{1}{\lambda} - \frac{\Pr}{(4-2\Pr)}\right\}$$

$$a_{13} = -\frac{2\mathrm{Br}\alpha^2(A+\lambda)\left(1+\sqrt{1+4\lambda}\right)}{\lambda\left(\alpha+\sqrt{K^*}\right)\left\{2\alpha+\sqrt{K^*}\left(1+\sqrt{1+4\lambda}\right)\right\}}$$

$$a_{14} = \left(\frac{3+\sqrt{1+4\lambda}}{2}\right)^2 - \Pr\left(\frac{3+\sqrt{1+4\lambda}}{2}\right) - \Pr\lambda$$

$$a'_{15} = A\Pr\left\{\frac{a'_{11}}{\lambda} - \frac{2a_{12}}{(4-2\Pr-\Pr\lambda)} - \frac{a_{13}}{a_{14}}\left(\frac{3+\sqrt{1+4\lambda}}{2}\right)\right\}$$

$$a_{16} = -\frac{\left(\alpha+\sqrt{K^*}\right)^2 a_{13}^2}{4\mathrm{Br}\alpha^2}$$

$$a_{17} = \frac{A\Pr a_{13}}{a_{14}}\left(\frac{3+\sqrt{1+4\lambda}}{2}\right) + \frac{2\mathrm{Br}A\alpha^2(A+\lambda)\left(1+\sqrt{1+4\lambda}\right)}{\lambda^2\left(\alpha+\sqrt{K^*}\right)\left\{2\alpha+\sqrt{K^*}\left(1+\sqrt{1+4\lambda}\right)\right\}}$$

$$a_{18} = \frac{2A\Pr a_{12}}{(4-2\Pr-\Pr\lambda)} - \frac{\mathrm{Br}A^2\alpha^2}{\lambda^2\left(\alpha+\sqrt{K^*}\right)^2}$$

$$a_{19} = (2-\Pr)\left(1+2\lambda+\sqrt{1+4\lambda}\right)$$

$$a_{20} = \left(\frac{3+\sqrt{1+4\lambda}}{2}\right)^2 - \Pr\left(\frac{3+\sqrt{1+4\lambda}}{2}\right) - 2\lambda\Pr$$

Entropy generation Analysis

The velocity and the temperature fields are utilized to compute entropy generation. The local volumetric rate of entropy generation SG is given as follows.

$$S_G = \frac{\kappa}{T_\infty^2}\left(\frac{dT}{dy}\right)^2 + \frac{\mu}{T_\infty}\left(\frac{du}{dy}\right)^2 \qquad (2.4.1)$$

The equation (2.4.1) reveals that entropy is generated by two sources. Firstly, heat transport across the boundary layer contributes to entropy creation; secondly, frictional fluid friction generates local entropy. Entropy generation rate is defined in terms of the characteristic generation rate (SG0), dimensionless temperature difference (), as well as the non-dimensional entropy generation Ns.

$$S_{G0}=\frac{q^2}{T_\infty^2\kappa}\ ,\quad \omega=\frac{V_0T_\infty\kappa}{qv}\quad \text{and}\quad N_s=\frac{S_G}{S_{G0}}$$

$$N_s=\frac{S_G}{S_{G0}}=\left(\frac{d\theta_1}{d\eta}+\varepsilon e^{\lambda t^*}\frac{d\theta_2}{d\eta}+\varepsilon^2e^{2\lambda t^*}\frac{d\theta_3}{d\eta}\right)^2+Br\omega\left(\frac{df_1}{d\eta}+\varepsilon e^{\lambda t^*}\frac{df_2}{d\eta}\right)^2$$
$$=HTI+FFI$$

$$HTI=\left(\frac{d\theta_1}{d\eta}+\varepsilon e^{\lambda t^*}\frac{d\theta_2}{d\eta}+\varepsilon^2e^{2\lambda t^*}\frac{d\theta_3}{d\eta}\right)^2 \text{ stands for heat transfer irreversibili}$$

and

$$FFI=Br\omega\left(\frac{df_1}{d\eta}+\varepsilon e^{\lambda t^*}\frac{df_2}{d\eta}\right)^2 \text{ stands for fluid friction irreversibility.}$$

Global entropy G_{Ns} is computed by integrating the local entropy and is obtained as follows

$$G_{N_s}=\int_0^{\eta_\infty}N_s d\eta \qquad (2.4.2)$$

RESULTS AND DISCUSSION

Figure 2.2 demonstrates that as decreases, velocity increases. Figure 2.3 shows that velocity increases as permeability K* increases. Figures 2.4 illustrate that velocity increases as t* and increase.

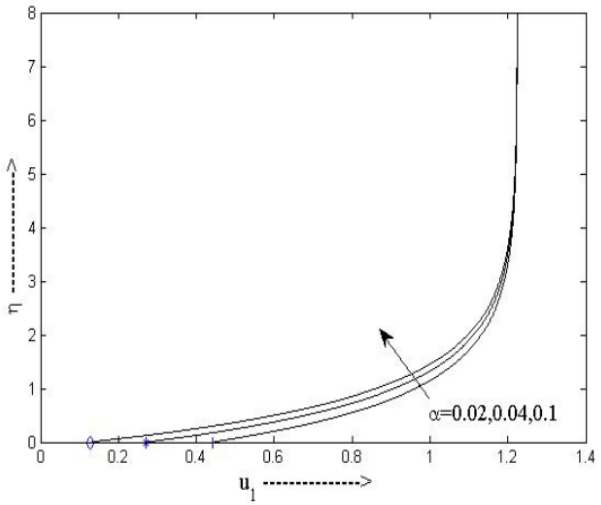

Figure 2.2 : Velocity profiles for varying α,for ε=0.05,A=0.1,t*=1,K*=0.0001,λ=1.5,Pr=0.9,ω=0.6,Br=10

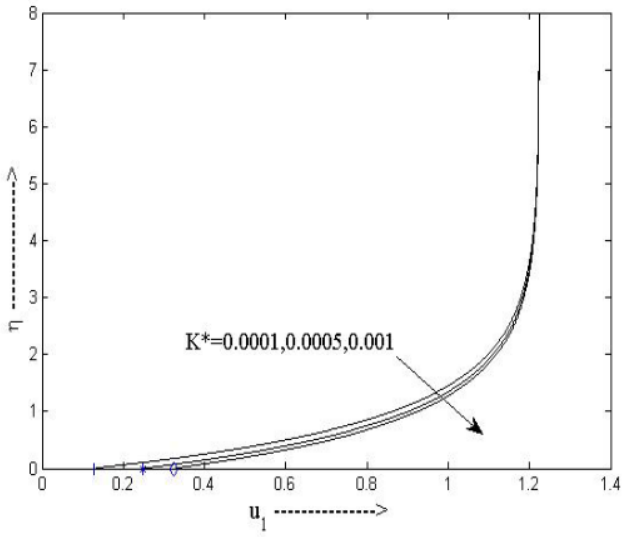

Figure 2.3 : Velocity profiles for varying K*,for ε=0.05,A=0.1,α=0.1,t*=1,λ=1.5,Pr=0.9,ω=0.6,Br=10

CONCLUSION

Numeral simulation modelling in heat transfer and fluid dynamics had attracted a lot of automated software interest. To simulate transient and steady-state models using boundary conditions of fluids, this study has provided a concept for layering the inputs depending on density. A variety of numerical methods have been used to describe various aspects of heat and mass transfer as well as fluid mechanics in the current work. FEM and BEM are used to demonstrate how these methods can be used to solve real-world heat and mass transfer and fluid mechanics problems in engineering. The validity and convenience of solution of several numerical methods have been evaluated for further engineering applications. Fluid flow arrangements have been studied extensively using mathematical models and simulations. Because of the fluid dynamic equations' scale neutrality; it is now possible to run simulations that produce results that are applicable to devices of any size. In terms of time, resources, and ease, this technique has proven to be more favourable than experiments with real-world systems for the existing or proposed systems. Fluid dynamics are found in practically every natural and industrial event, and this is why it is so important to understand them. Many natural, industrial, and technological processes rely on fluid flow and heat transmission. Numerous fields, such as astrophysics, geophysics, internal combustion engines, heating and air conditioning systems, electronics cooling systems, oceanography and atmospheric sciences as well as the circulatory and metabolic systems, biological sciences and waste disposal all benefit from research into thermo fluidic systems.

REFERENCES

1. Abdelkhalek, M.M., Heat and Mass transfer in MHD free convection from a moving permeable vertical surface by a perturbation

technique, Communications in Nonlinear Sciences and Numerical Simulationvol.14(5), pp. 2091-2102, (2009).
2. Abel, M.S. and Mahesha, N., Heat transfer in MHD viscoelastic fluid flow over a stretching sheet with variable thermal conductivity, nonuniform heat source and radiation, Appl. Math. Modelling, vol. 32, pp. 1965–1983, (2008).
3. Ackerberg, R.C.,The viscous incompressible flow inside a cone, J. Fluid Mech., vol. 21, pp. 47-81, (1965).
4. Ahmed, J., Shahzad, A., Begum, A. ,Ali , R. and Siddiqui, N., Effects of inclined Lorentz forces on boundary layer flow of Sisko fluid over a radially stretching sheet with radiative heat transfer, Journal of the Brazilian Society of Mechanical Sciences and Engineering , DOI: 10.1007/s40430-017-0759-z, vol.39, No.8, pp.3039-3050, (2017).
5. Aiboud, S. and Saouli, S., Entropy analysis for viscoelastic magnetohydrodynamic flow over a stretching surface, International Journal of Non Linear Mechanics, vol. 45, pp. 482–489, (2010).
6. Al-Odat M.Q., Damesh R.A. and Al-Nimr M.A., Effect of magnetic field on entropy generation due to laminar forced convection past a horizontal flat plate, Entropy, vol. 4, pp. 293-303, (2004).
7. Aman F., IshakA.and Pop, I., Magnetohydrodynamicstagnationpoint flow towards a stretching/shrinking sheet with slip effects, International Communications in Heat and Mass Transfer, vol.47, pp.68–72, (2013).
8. Asatur, K.G. and. Kolton, G.A, Laminar boundary-layer in an axisymetric convergent duct, Fluid Mechanics (soviet Research), vol. 20, pp. 24-27, (1991).
9. Awais, M., Hayat ,T., Mustafa, M., Bhattacharyya, K. and Farooq, M.A., Analytic and numeric solutions for stagnation-point flow with melting, thermal-diffusion and diffusionthermo effects, Int. J. Numer. Meth. Heat Fluid Flow, vol.24, No.2 , pp.438-454, (2014).
10. Awais, M., Hayat T. and Alsaedi A., Investigation of heat transfer in flow of Burgers' fluid during a melting process, Journal of the Egyptian Mathematical Society, vol.23, pp.410–415, (2015)

Corresponding Author

Ritika*

Research Scholar, Sunrise University